Dispatchability of Solar Photovoltaics from Thermochemical Energy Storage

R. Fernández [a], C. Ortiz [b,*], Chacartegui R. [a], Valverde J.M. [b], Becerra J.A. [a]

[a] Escuela Técnica Superior de Ingeniería, Universidad de Sevilla, Camino de los descubrimientos s/n, 41092 Sevilla, España
[b] Facultad de Física, Universidad de Sevilla, Avenida Reina Mercedes s/n, 41012 Sevilla, España,
[*] Corresponding author (C. Ortiz): cortiz7@us.es; t:(+34) 655783930

ABSTRACT

Solar photovoltaics (PV) plants are today a competitive alternative to power plants based on fossil fuels. Cost reduction in PV modules, scalability (from kW to MW) and ease of installation of PV plants are enabling a rapid expansion of the technology throughout the world. Nevertheless, PV dispatchability still remains as the major challenge to be overcome due to intrinsic variability of solar energy. Most of the current PV facilities at large scale lack energy storage while those with storage systems rely on expensive batteries. Batteries are based on elements such as nickel, lithium or cadmium whose scarcity hinder the sustainability of batteries for storing energy in the large scale. This manuscript presents a novel concept to integrate thermochemical energy storage in PV plants. Furthermore, the concept is also directly adaptable to wind power plants in order to store surplus energy. In particular, this paper analyses the suitability of the Calcium-Looping (CaL) process as thermochemical energy storage system applied to large scale PV facilities. The PV-CaL integration works as follows: a part of power produced in the PV plant provides electricity to the grid while the rest is used to supply heat to carry out the calcination of $CaCO_3$. After calcination, the products of the reaction (CaO and CO_2) are stored separately. When power production is required, the stored products are brought together in a carbonation reactor wherein the exothermic reaction releases energy for power production. The overall system is simulated in order to estimate the process behaviour and results show that storage efficiencies of ~40% can be achieved. Moreover, an economic analysis is developed to compare the proposed system with batteries. Due to the low price of natural CaO precursors such as limestone and the longer lifetime of equipment than batteries, the CaL process can be considered as a suitable alternative to increase dispatchability in PV plants. Moreover, limestone is abundant and non-toxic, which is an essential requirement for the storage of energy in massive amounts.

KEYWORDS

Global warming, Renewable energies, Photovoltaic (PV), Thermochemical energy storage (TCES), Calcium looping (CaL), dispatchability

1. INTRODUCTION

Solar photovoltaics (PV) plants are considered as one of the most promising markets in the field of renewable energy [1], with a PV market growth by 50% in 2016 [2]. The size of PV Plants varies depending on the application [3]: from Pico PV systems of few watts used for off-grid basic electrification, to Grid Connected Centralized systems in the range of MWs [4]. The scalability (from kW to MW), ease installation and cost reduction are enabling a fast growing of the PV installed power all around the world, representing the third worldwide largest

renewable source after hydro and wind [5]. Technical improvements and economy of scale have resulted in a significant cost reduction of solar photovoltaic (PV) modules, and an intense global growth of PV industry [6]. Nevertheless, dispatchability still remains as a major challenge to be solved due to intrinsic variability of solar energy. The intermittent nature of PV can also cause oscillations in the power system's voltage and frequency, which create new challenges for the integration of PV in the electric power system [7]. Coupling grid connected PV plants to energy storage systems is a possible solution to solve this problem [8], making thus possible to stabilize electricity supply and move production to high prices in peak periods.

Batteries -Electrochemical Energy Storage Systems (ECES)- have been postulated as the best positioned systems for solving dispatchability issues for renewable energy sources (RES) integration. Johan et al. [9] report the energy efficiency of different batteries technologies, which goes from 85-95% efficiency for Li-ion batteries to 60-65% for PSB technology, which is currently the most appropriate technology for large scale plants. However, and despite the huge expansion of batteries in market [1], the commercial expansion of batteries still faces great challenges for large scale energy storage. Batteries based on materials such as Lithium, Nickel or Cobalt, whose scarcity and environmental impact compromise the technical and economic viability of this technology for massive energy storage around the world. Moreover, the cost of the batteries is another major drawback, around 300-550$/kWh [10], which is one order of magnitude over thermal storage systems.

Recently Tesla has built a Li-ion battery (100MW/129MWh) tom demonstrate large scale penetration of RES in Australia [11]. By 2030 the expected PV installed capacity will be nine times higher than in 2013 [10]. In this line, Geth el al. [12] highlight the necessity of large scale storage systems for integrating non-dispatchable renewable energy and exclude battery storage as a realistic candidate to provide bulk energy storage capabilities. In addition to resource scarcity and cost, another major challenge of batteries is to prolong the lifetime of the system. Because of the variability of solar input, batteries are subjected to continuous charge and discharge cycles, which increases their complexity and cost for large scale facilities [10]. On the other hand, pumped hydro storages, which accounts for 99% of the total installed energy stored, is a feasible solution for the massive storage of energy [13]. However, the application of this technology is constrained to special locations with high altitude gradients.

This manuscript presents a novel concept to integrate Thermochemical Energy Storage (TCES) systems in PV plants, as a sustainable and large-scale storage system. Among the TCES systems, the Calcium-Looping (CaL) process, based on the multicyclic calcination/carbonation of $CaCO_3$ has been selected in this work. The CaL process has been recently analysed to enhance dispatchability in Concentrating Solar Power (CSP) plants [14–17]. Main advantages of the CaL process for TCES, are: i) the high energy storage density of the system [18], the high turning temperature of the carbonation reaction [19], which allows using high-efficiency power cycles, and iii) the low cost, wide availability and non-toxicity of natural CaO precursors such as limestone or dolomite.

Despite that converting electric power to thermal would seem counterproductive from a thermodynamic point of view, there are several ambitious projects, such as the Google's Project Malta [20], and publications [21] exploring this possibility as alternative to batteries. Storing electricity in the form of heat is lately gaining attention due to the very low prices of electricity production achieved in PV plants and the increasing surplus of electricity produced that cannot be used. Just in California 10 GWh of wind and solar generation is being wasted over the 24-hour period due to curtailment [22].

The so-called Electrical Energy Storage – Calcium looping (EES-CaL) system is based on using the power produced for a PV plant to provide heat by Joule effect for carrying out the calcination endothermic reaction, whose products CaO and CO_2 are stored separately by long periods. When energy is required, the stored products are sent to another reactor where by means of the carbonation exothermic reaction is released the stored energy in the chemical bonds. The system is connected to the centralized power system to export electrical power generated in the power block for the discharge of the cycle. Thermal to electrical efficiencies higher than 40% can be reached in the integration of the CaL process in CSP plants [23,24]. The EES-CaL system allows exploiting several storage management strategies by just configuring the charging and discharging cycles of the TCES and integrating them with the electrical supplier system (PV plant) and the power system.

This document is structured as follows: firstly, the novel concept for EES based on CaL technology (EES-CaL) is described with particular focus on the PV integration (PV-CaL). Later on, the system is simulated to analyze the daily behavior for each month of the year. Main results are discussed highlighting the importance of managing storage tanks. A brief discussion on economic issues is also introduced to complete this first approach to the EES-CaL concept.

2. CONCEPTUAL EES-CAL SYSTEM FOR PV PLANTS

Figure 1 illustrated the conceptual scheme for the EES-CaL system in PV plants (PV-CaL). The system is composed by two well-differentiated and independent charging and discharging cycles with solid storage tanks and CO_2 vessel. The CaL process scheme is based on a recent work [24] where interested readers can find further details on the configuration. The EES–CaL process begins by activating the charging cycle, where the endothermic calcination of limestone ($CaCO_3$) takes place. During the charging cycle, electric power from PV is transformed to thermal power by electric heaters coupled to the calciner. Thus, a part of the electrical power generated in the PV system feeds the EES. The calciner, which may be configured as a Fluidized Bed (FB) or as an Entrained- Flow (EF) reactor, operates under atmospheric pressure at 950 ºC to ensure fast decomposition of $CaCO_3$ [15]. In this conceptual approach, full calcination is assumed [17]. Thermal power provided to the calciner is used for increasing the solids temperature up to the reaction conditions and to provide the calcination enthalpy according to Eq 1.

$$CaCO_{3\,(s)} + \Delta H_r \rightarrow CaO_{(s)} + CO_{2\,(g)} \qquad \Delta H_r = 178\ \frac{kJ}{mol} \tag{1}$$

The $CaCO_3$ entering the calciner is controlled depending on the power provided by the PV system. The higher the power to the calciner the higher amount of $CaCO_3$ entering the reactor from the solids storage tank. The CaO produced during calcination is directly stored while the CO_2 is passed through a heat exchanger before being compressed. First, the CO_2 is sent to a cyclonic gas-solid preheater where $CaCO_3$ entering the reactor is heated. These preheaters are a well-known technology in cement plants [25]. Later, the CO_2 is sent to a heat recovery within a power cycle (e.g. Stirling Engine). Another option could be using its sensible heat for thermal applications within the plant. The CO_2 stream is further cooled before pressurizing it up to 75 bar [26] by means of an intercooling compressor. The charging cycle ends once the CaO and CO_2 streams produced in the calciner are stored.

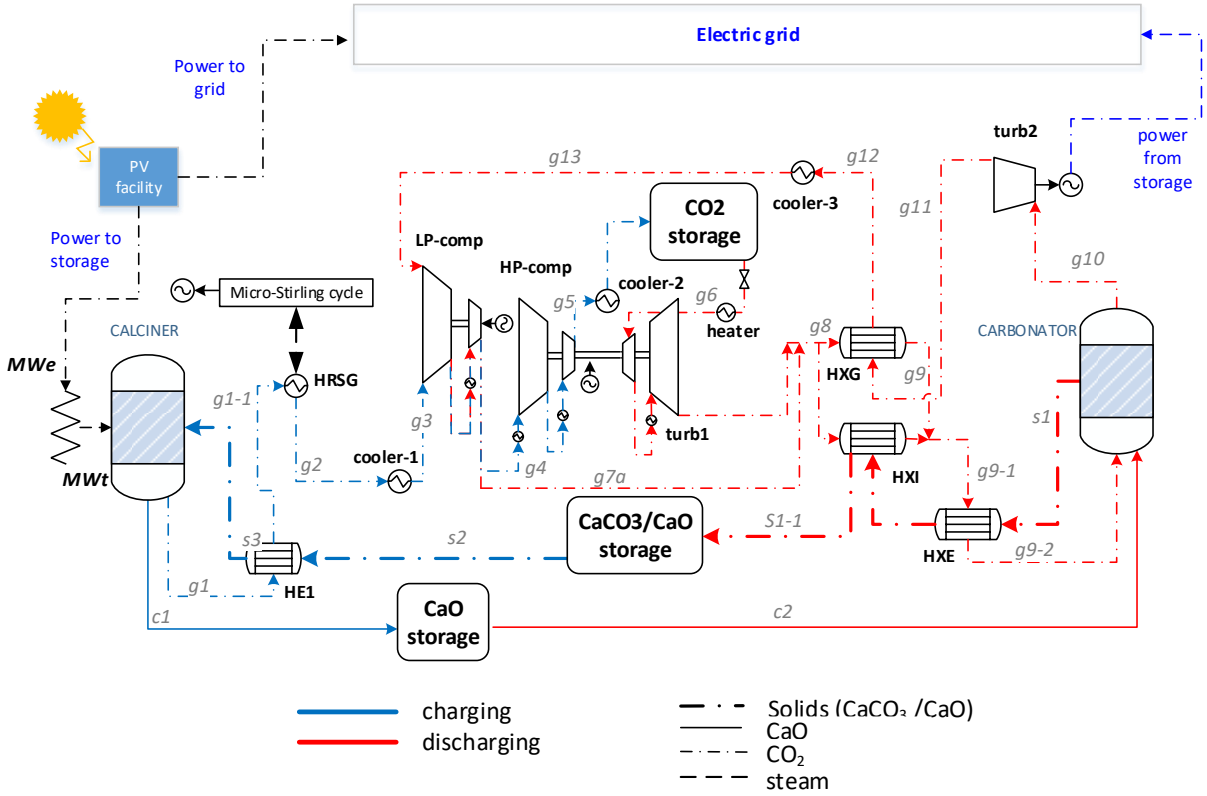

Figure 1. Conceptual scheme for PV-CaL

The $CaCO_3$ produced in the carbonator is stored to start a new cycle. The main challenge for the CaL process is the progressive decrease of CaO conversion (X) as the number of cycles increases until reaching a residual value. This loss of activity is mainly dependent on temperature, pressure and gas composition in both carbonator and calciner reactors and can be largely mitigated by choosing appropriate conditions [27,28].

The discharging cycle begins when there exists an interest in generating electrical power which has been previously stored during the charge cycle. To activate the discharge cycle for power production, CO_2 and CaO from the storage are sent to the carbonator reactor, where the exothermic carbonation reactions occurs. To achieve the desired operation at the exothermic reactor, the control system acts over the mass flow rate of CaO exiting the storage tank, which is an independent variable as input for the discharge cycle. In turn, the CaO mass flow rate entering the carbonator determines the total flow rate of CO_2 coming from the storage vessel. The CO_2 at low temperature is passed through a heater before passing it to a turbine to match the carbonator pressure (plus the pressure losses in the CO_2 heat exchangers). After this, the CO_2 stream is passed through a heat exchanger network in order to enter the carbonator at the highest temperature (Figure 1). The amount of CO_2 entering the carbonator is well above the stoichiometric need which allows using the non-reacting CO_2 as heat carrier fluid. As shown in Figure 1, the CO_2 exiting the carbonator at high temperature and pressure and evolves through a thermal turbine to produce power. In this direct integration the whole system, including charge and discharge processes, constitutes a closed CO_2 Brayton regenerative cycle with elements decoupled in time.

One of the main challenges of CaL process in the progressive CaO deactivation as the number of cycles increases. Previous works have shown however that CaO deactivation is highly dependent on the conditions in the calciner and carbonator reactors (temperature, total pressure, CO_2 partial pressure) as well as on the CaO precursor and their physical properties (particles

size, impurities, etc.) [29,30], and they depend on the application. Thus, a residual CaO conversion as large as X=0.5 may be achieved for carbonation under 100% CO_2 atmosphere and calcination at 725 ºC in absence of CO_2 when using natural limestone with particle size smaller than 45μm [31] Pore plugging limits conversion for larger particles, which in that case reaches a residual value of only X=0.2. [16,17]. A conservative baseline value of X=0.15 is assumed in the present work for simulating the PV-CaL integration at stationary conditions. Other assumptions about the CaL process scheme have been considered in this work. Turbomachinery efficiency, pressure drops values as well as heat exchangers modelling are presented in [24].

3. CASE OF STUDY

To illustrate the concept an application of integrated PV-CaL system is developed in this section.

3.1. PV facility

A detailed simulation of a PV facility located in Seville (Spain) has been performed by using System Advisor Model (SAM) [32]. The PV system is sized for generating 20 MW in DC under 1,000 W/m^2 of total irradiance and cell temperature of 25 ºC. The PV module selected for the PV system is *Sun Power SPR-E19-245* (main characteristics are presented in Table 1) while the selected inverter is *SAM America: CS750CP-US-342V (*Table 2).

Table 1. Module characteristics at reference conditions

Nominal Efficiency	19.169	%
Maximum power (Pmp)	245.025	W_{dc}
Maximum power voltage (Vmp)	40.5	V_{dc}
Maximum power current (Imp)	6.1	A_{dc}
Open circuit voltage (Voc)	48.8	V_{dc}
Short circuit current (Isc)	6.4	A_{dc}
Module area	1.244	m^2

Table 2. Inverter characteristics at reference conditions

Maximum AC power	770000	W_{ac}
Maximum DC power	785145	W_{dc}
Power consumption during operation	1992.12	W_{dc}
Power consumption at night	364.7	W_{ac}
Nominal AC voltage	342	V_{ac}
Maximum DC voltage	1000	V_{dc}
Maximum DC current	1600	A_{dc}
Minimum MPPT DC voltage	545	V_{dc}
Nominal DC voltage	617.789	V_{dc}
Maximum MPPT DC voltage	820	V_{dc}
European weighted efficiency	98.122	%

A number of 26 inverters is required for the system size, 20 MW_{dc}, with a maximum DC power by inverter of 785.14 kW_{dc} (Table 2). Thereby the DC-AC ratio would be 0,999 at reference conditions. The number of PV modules series-connected (modules per string) is given by the average DC voltage in the inverter (772.5 V_{dc}) and the V_{oc} of modules (Table 1). Thus, a total of 16 modules per string have been calculated for the system. The maximum number of parallel strings for the system is calculated as the maximum DC current in the system (maximum DC

current in inverter multiplied by the total number of inverters) divided by the short circuit current in the PV module (I_{sc}). As a result, a maximum of 6500 strings in parallel is obtained. Considering 20MWdc of sizing power of the system and a configuration with 16 modules per string, a total of 5100 strings in parallel are required, resulting in 81600 modules. The final configuration of the system and main parameters at reference conditions are shown in Table 3:

Table 3. PV Power Plant configuration at reference conditions

Modules			Inverters		
Nameplate capacity	19994.04	kW_{dc}	Total capacity	20020	kW_{ac}
Number of modules	81600		Total capacity	20413.77	kW_{dc}
Modules per string	16		Number of inverters	26	
Strings in parallel	5100		Maximum DC voltage	1000	V_{dc}
Total module area	101510.4	m^2	Minimum MPPT voltage	545	V_{dc}
String V_{oc}	780.8	V	Maximum MPPT voltage	820	V_{dc}
String V_{mp}	648	V	Actual DC to AC ratio	0.9987033	

The operation of this PV facility located in Seville has been simulated for one-year. It results in an annual generation efficiency of 18.16%, with annual solar irradiance of 180.44 MWh/year and annual generation of 32.77 MWh/year. Figure 2 shows the results of the simulation along the year (a) and in the peak power day (b).

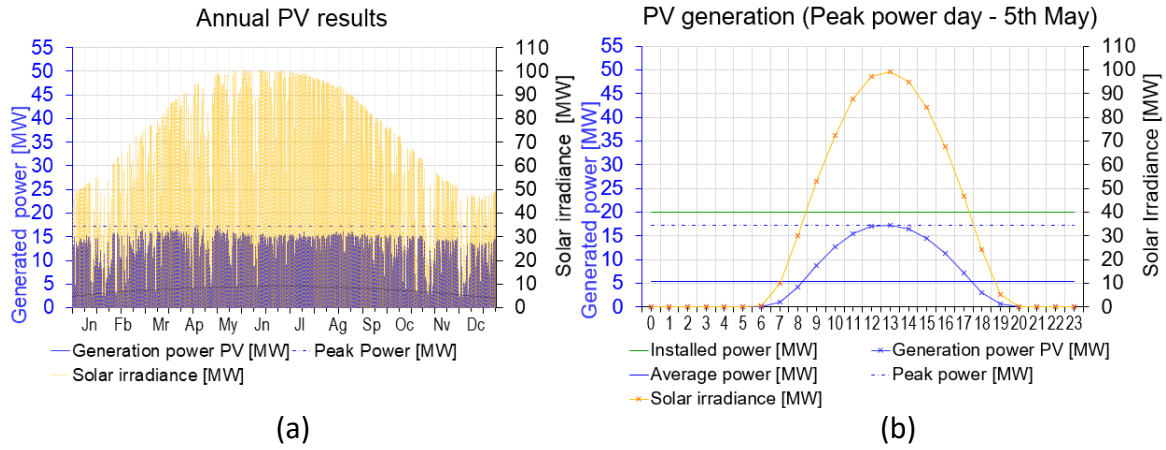

Note the scales difference between left and right vertical axes.

Figure 2. Simulation results: a) Annual results b) Peak power day results

Figure 2 shows the characteristic intermittent power production linked to seasonal and daily intermittence in solar resource. The PV facility is designed for 20 MW modules capability (under reference conditions), but peak power for the simulated year is 17.3 MW (Figure 2 (a)) since reference conditions and 1000W/m^2 of solar irradiance (nominal conditions) have not been achieved simultaneously to generate 20MW of PV power. The power generation average value is 3.74 MW, which is equivalent to 1638 full-load-hours throughout the year.

3.2. PV-CaL process simulation (base case)

The PV-CaL integration schematized in Figure 1 has been simulated in order to analyse its potential as electric energy storage system. First, a base case is defined. It uses 5 MW_e of electric power produced by the PV system in the CaL process. In the charging period, the use of electric heaters coupled to the calciner allows the calcination of 1.86 kg/s of $CaCO_3$. Taking into account that CaO conversion in the carbonation is not complete, in addition to $CaCO_3$, a certain amount

of non-reacted CaO from the carbonator enters the calciner and therefore the total amount of solids would be 7.74 kg/s. For the base case analysis, it is assumed that solids exit the storage vessel at 690 ºC. Once calcination occurs, 0.82 kg/s of CO_2 and 6.93 kg/s of CaO are sent to their respective storage tanks. Within this base case, the discharging process is modelled assuming that all the previously stored CaO is sent to the carbonator for power production. Table 4 and 5 show main streams data and energy balance of the system results. Nomenclature corresponds to the one used in Figure 1.

Table 4. Main streams data for the PV-CaL integration (base case, 5 MWe from PV to CaL storage)

ID	P [bar]	T [^{0}C]	ṁ [kg/s]	ID	P [bar]	T [^{0}C]	ṁ [kg/s]
s1	3.5	900	7.74	**g5**	75.75	123.65	0.82
s1-1	1.14	689.20	7.74	**g5-2**	75	25	0.82
s2	1.14	689.60	7.74	**g6**	74.25	130	0.82
s3	1.11	719.69	7.74	**g7a**	3.85	78.36	18.01
c1	1	950	6.93	**g8**	3.85	76.80	18.83
c2	1	950	6.93	**g9**	3.66	702.62	18.83
g1	1	950	0.82	**g10**	3.5	900	18.02
g1-1	0.97	719.76	0.82	**g11**	1	718.18	18.02
g2	0.97	70	0.82	**g12**	0.95	91.99	18.02
g3	0.96	40	0.82	**g13**	0.94	40	18.02

The CO_2 stream exits the calciner at high temperature (950 ºC). This high temperature stream is used to increase the temperature of the incoming solids up to 720 ºC and to produce extra power in the Stirling engine. This hot CO_2 stream can be used for recovering energy integrating it with a thermal engine aiming to increase the global cycle efficiency and reducing the cooling demand of the system. After cooling, the CO_2 stream is compressed up to 75.75 bar before entering the storage tank. Once calcination take places, both the CO_2 and CaO streams previously produced in the calciner are sent to the carbonator reactor. In the discharging step, CO_2 at 75 bar and 25ºC is circulated through a heater increasing its temperature up to 130 ºC before passing through the secondary CO_2 turbine. After passing through the heat exchanger network, this stream arrives the carbonator at 753ºC. Table 5 shows the energy balance of the plant.

Table 5. Energy balance for the PV-CaL integration (base case, 5 MW_e from PV to storage)

	Parameter	Charging step	Discharging step
Solar thermal power (MW_{th}) from PV to storage		5	0
Heat exchangers thermal Power (MW_{th})	HRSG	0.58	-
	HE-1	0.23	-
	COOLER-1	-0.02	-
	HP-COMP (intercooler)	-0.25	-
	COOLER-2	-0.22	-
	HEATER	-	0.23
	TURB1 (interheater)	-	0.08
	COOLER-3	-	-0.84
	HXG	12.41	12.41
	HXE	1.17	1.17
	HXI	0.50	0.50
	LP-COMP (intercooling)	-	-1.23
Power inlet (MW_e)	CO_2 storage turbine (TURB1)	-	0.11
	Main CO_2 turbine (TURB2)	-	4.02
	Externally heated engine-Stirling engine	0.12	-
	CO_2 storage compressor (HP-COMP)	-0.29	-
	Main CO_2 compressor (LP-COMP)	-	-1.84
	Auxiliaries heat calciner	-0.004	-
	Auxiliaries solids transport calciner	-0.08	-
	Auxiliaries solids transport carbonator	-	-0.08
W_{net}	$\dot{W}_{net,charge}$ (MWe)	-0.25	-
	$\dot{W}_{net,discharge}$ (MWe)	-	2.21
	Overall plant efficiency (η)	**39.21%**	

Table 5 includes main results from the energy balance in the plant. It shows that with the integration 14.66 MW_{th} have been recovered from the hot streams and integrated into the process, thus increasing the overall efficiency of the plant. Otherwise, there is still a need for extra cooling and heating power of 2.56 MW_{th} and 0.31 MW_{th} respectively. Global generation in the system is 4.25 MW_e by means of two CO_2 turbines allocated in the discharging cycle and an externally heated engine (for this size a Stirling engine is considered) that recovers thermal power from the hot CO_2 stream exiting the calciner. Energy consumption in the plant (2.28 MW_e) is mainly due to compressors consumption (2.12 MW_e). Note that net energy in the charging process is negative because of the CO_2 compression. As a result of this energy balance, the net generation in the charging and discharging cycle are 2.21 MW_e (net generation) and -0.25 MW_e (net consumption), respectively when the solar thermal power entering in the calciner is 5 MW_e. Considering net electric generation in the system for a given thermal power entering the charging cycle, the overall efficiency of the system is 39.21%.

4. PV-CaL process design

Once the PV-CaL process configuration has been analyzed for the base case, this section aims at studying the daily behavior of the system by considering a quasi-stationary simulation in an

hourly basis. Modelling has been carried out without considering off-design conditions at this preliminary stage. PV generation in a typical monthly day (hourly generation considered as the average value of hourly generation for every day of the month) is used as representative of the month behavior. Power generation in the PV facility is exported to the grid with a maximum power of 2.5 MW_e. When generation exceeds this limit, the surplus electricity is sent to the CaL charging cycle to initiate calcination and storage of reaction products.

In the analysis, a 24h constant discharging -power production- strategy is considered. Thus, the amount of constant power production from storage in each day depends on weather conditions. The surplus electricity generated in the PV facility over the exported to the grid is used for the charging cycle of the storage system. The amount of CaO and CO_2 used to produce surplus generation hours is distributed along the day to balance levels in the daily operation. Figure 3(a) summarizes the energy balance in the PV-CaL system. As result of the energy storage process along a typical July day, energy is stored for 11 hours, -from 9:00 to 19:00h- and then power production continues almost constant the rest of the day. Net generation during charging hours in the CaL system is negative because of the CO_2 compression (Table 5). Nevertheless, the net generation during discharging hours remains constant at 2.48 MW_e. The global performance of the system, which is calculated as the PV-CaL net generation divided by the total PV-generation, is 56.5% and represents a loss of a 44.5% of the total PV-generation due to the storage system. Figure 3 (b) shows a plot the daily duration curve of the PV facility and the PV-Cal system and illustrates the purpose of this strategy, which is conceived to shift intermittent RES generation into almost even and controlled generation.

The PV-CaL system net generation takes into account net generation during discharging hours and PV exported during charging hours. This result is the total energy exported to the grid from the integrated PV-CaL system.

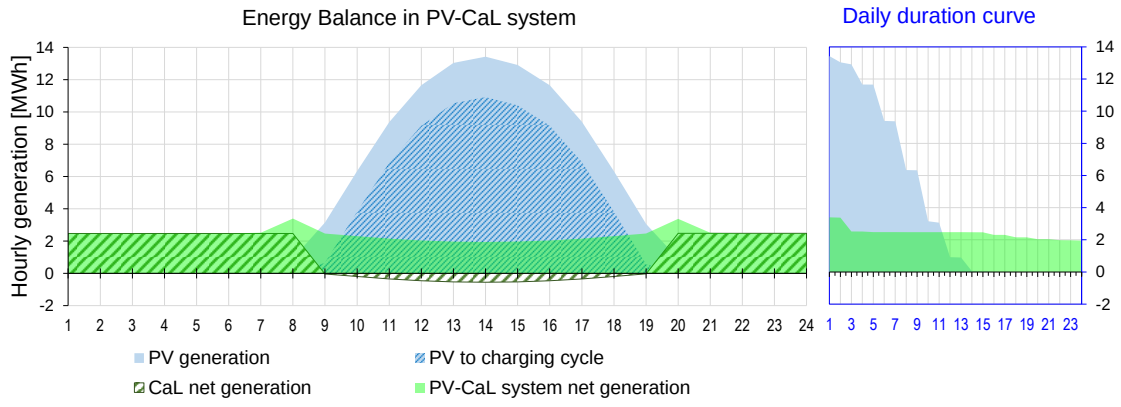

(a) (b)

Figure 3. PV-CaL system performance: a) Energy balance in the PV-CaL system. Hourly results; b) Daily duration curve

Figure 3(a) summarizes the energy balance in the PV-CaL system. The performance of the CaL system obtained is the same than in the base-case, 39.2% (Table 5), since all products from calcination are used in the carbonator. Otherwise, the global performance of the system, which is calculated as the PV-CaL net generation divided by the total PV-generation, is 56.5% and represents a loss of a 43.5% of the total PV-generation due to the storage system. Figure 3 (b) shows a plot the daily duration curve of the PV facility and the PV-Cal system and illustrates the purpose of this strategy, which is conceived to shift intermittent RES generation into almost even and controlled generation.

Storage tanks management is a crucial issue of the PV-CaL system. Figure 4 shows the daily evolution of solids ($CaCO_3$ + CaO), CaO and CO_2 tanks. According to the results, storage capacities of around 360 tonnes of CaO and 45 tonnes of CO_2 are needed.

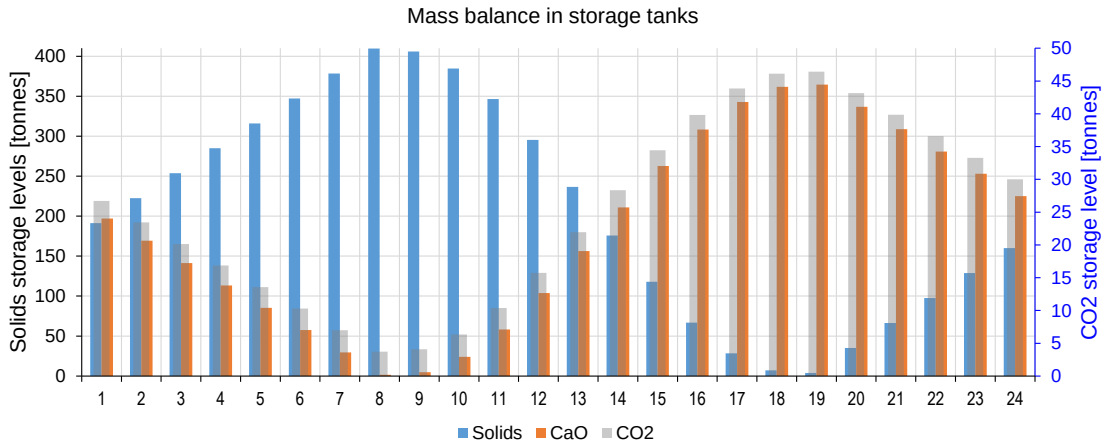

Figure 4. PV-CaL performance. Mass balance in storage tanks

Table 6 shows main results of the daily simulation for each month. 24h- hours constant production is in the range of 2.48 MW_e in July to 1.19 MW_e in December, with an annual average of 1.85 MW_e. This average value is selected as design power production value to evaluate operation of the system throughout the year.

Table 6. Base PV-CaL generation. Monthly results

Month	**Power generation [MW]**		**Energy balance - Generation [MWh]**				**Global PV-CaL performance**	
	PV threshold	PV-CaL discharge	PV to grid)	PV to storage)	CaL to grid	PV-CaL system to grid	C/D [h]	Operation Performance
JAN	1.35	1.33	12.18	45.06	17.69	29.87	9/15	52.17%
FEB	1.5	1.47	14.28	49.98	19.60	33.88	9/15	52.72%
MAR	2.1	2.04	21.56	69.08	27.07	48.63	9/15	53.65%
APR	2	1.91	22.46	60.53	23.72	46.18	10/14	55.65%
MAY	2.3	2.30	26.97	67.71	26.53	53.5	11/13	56.50%
JUN	2.25	2.20	26.87	64.60	25.33	52.2	11/13	57.07%
JUL	2.5	2.48	29.40	72.83	28.55	57.95	11/13	56.69%
AGO	2.45	2.46	27.98	72.41	28.38	56.36	11/13	56.14%
SEP	1.95	1.88	20.66	63.79	25.01	45.67	9/15	54.08%
OCT	1.7	1.69	16.78	57.17	22.41	39.19	9/15	52.99%
NOV	1.2	1.19	10.66	42.87	16.81	27.47	8/16	51.31%
DEC	1.2	1.19	10.31	42.45	16.63	26.94	8/16	51.06%

5. PV-CaL process daily simulation

When the system is simulated on a representative day of December, the amount of products from the charging cycle is enough to allow generating 1.85 MWe almost constant during 19h, achieving a global efficiency in the operation of the system of 54.59%.

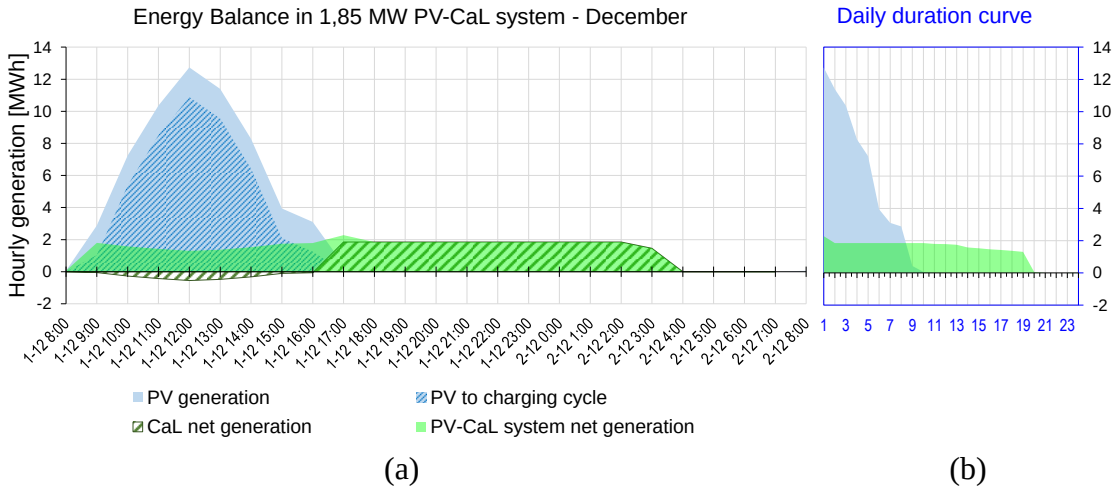

(a) (b)

Figure 5. PV-CaL 1.85MWe system – December: a) Energy balance in the PV-CaL system; b) Annual duration curve

Figure 5 shows the evolution of storage tanks levels along the simulated period. In this case, calcination products are fully consumed along the day and the system is balanced on a daily basis. This is the strategy set for this application but different ones can be considered taken into account the seasonal storage capacity of the CaL system. The minimum required storage capacities are 251.52 tonnes for solids, 26.49 tonnes for CO_2 and 225.03 tonnes for CaO.

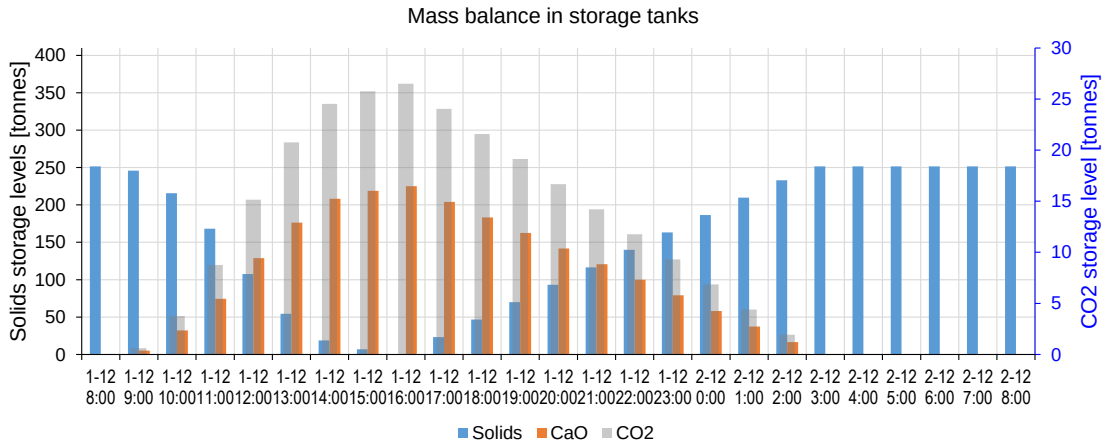

Figure 6. CaL 1.85MWe system – December. Mass balance in storage tanks

The opposite scenario is found on a representative of July (with a peak power capacity of 115.68 MWh/day). Figure 7 shows the performance of the system in this month. During the charging cycle (1.Jul: 9:00 h-19:00h) 454.56 tonnes of CaO are produced and stored before the discharging cycle (1.Jul: 20:00h-2.Jul: 8:00h), which consumes 244.04 tonnes of CaO, thus implying the necessity of extra-storage to address decoupled values of solids and gas streams production and consumption to maintain a strategy of constant power along the whole day. Figure 8 shows the mass balance in the PV-CaL system during the operation day. Calcination products are not totally consumed while the consumption of $CaCO_3$ in the calciner is not totally replaced in the discharging cycle thus reducing the level of solids storage tank at the end of the

operation day. This is because the selected operation strategy, which must be improved in order to minimize the storage size, and therefore the investment cost.

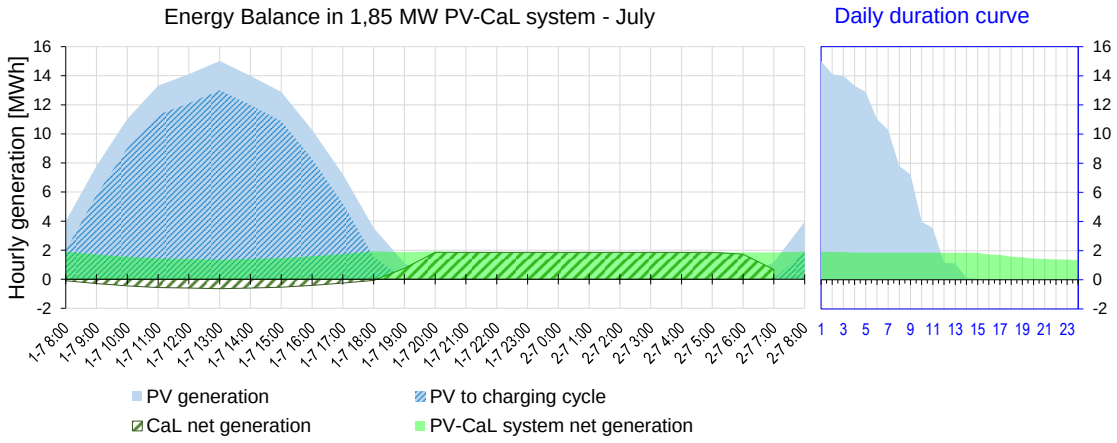

Figure 7. PV-CaL 1.85MWe system – July: a) Energy balance in the PV-CaL system; b) Annual duration curve

Figure 7 shows the mass balance in the PV-CaL system during the operation day. Calcination products are not totally consumed while the consumption of $CaCO_3$ in the calciner is not totally replaced in the discharging cycle thus reducing the level of solids storage tank at the end of the operation day.

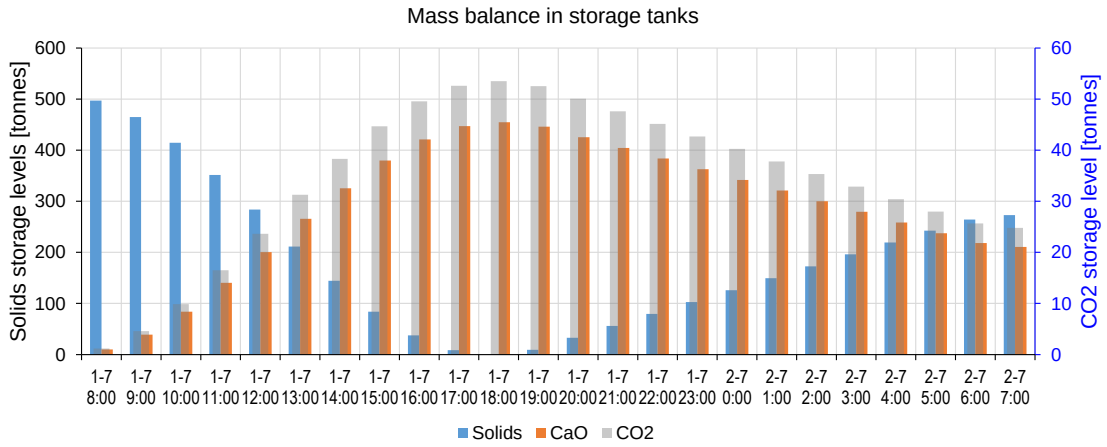

Figure 8. CaL 1.85MWe system – July. Mass balance in storage tanks

6. Economic and sustainability notes

A brief economic study has been carried out for the PV system simulated in the previous section. For storage system sizing the date of first of July has been selected. The aim of this section is to show the potential of the PV-CaL conceptual integration. According to the daily behaviour simulation, 91.18MWhe from the PV facility are charged in the storage system.

In order to estimate the PV-CaL system cost, the methodology proposed in [33] has been followed. Process equipment capital cost has been calculated by using Aspen Capital Cost Estimator [34]. Capital costs of the calciner and carbonator reactors have been estimated according to [35]. Table 7 shows the capital cost estimation for the CaL process as TCES.

Because of the novelty of the application and the design effort at this stage, a high contingency cost for the process (15%) and project (30%) has been assumed [33]. The owner cost, which includes feasibility studies, insurance, permitting, land, etc. has been estimated from [34]. Table 8 shows investment costs. For comparison, a generic batteries-based system is considered for the same size than the PV-CaL system. According to [10], the installed cost (including battery cells -whose cost is around 300-550$/kWh-, a power conversion system, a battery management system, etc.) of a Li-ion battery storage system currently available in the market is around 1200$/kWh, which yields a total cost for the simulated case of 109M€.

Table 7. Capital cost estimation for the proposed EES-PV-CaL configuration

Process equipment [M€]	25.28
Reactors	*12.03*
Storage Vessels	*2.77*
Heat exchangers	*2.45*
Turbomachinery	*5.95*
Solids conveying and separation	*0.47*
Electric heaters	*0.65*
Micro steam cycle	*0.96*
Supporting facilities [M€]	13.65
Piping	*3.09*
Civil	*0.62*
Steel	*0.13*
Instruments	*2.62*
Electrical	*1.98*
Insulation	*0.33*
Paint	*0.17*
Bare Erected Cost (BEC) [M€]	**38.93**
Engineering services [36] [M€]	1.75
EPC cost [M€]	**40.68**
Process contingencies [33] [M€]	6.1
Project contingencies [33] [M€]	12.2
Total plant cost [M€]	**58.98**
Owner cost [M€]	1.18
Total Overnight Cost (TOC) [M€]	**60.16**

As may be seen in Table 7, a notable cost reduction could be achieved by using the PV-CaL instead of the batteries-based PV. It shows the interest for further studies of this application at large scale level. As a novel technology, uncertainty about costs evolution for the EES- PV-CaL plant is high. To include into the analysis this uncertainty, a sensitivity analysis with random numbers has been carried out by considering a typical range of potential values for the main costs. Several criteria can be found in the literature for process and project contingencies for a CaL-based system [34,37,38]. Thus, a normal distribution for the process equipment cost (μ=25;σ=3) and uniform distribution for both process contingencies ([7-20%]) and project contingencies ([20-40%]) was considered. The sensitivity analysis results are shown in Figure 9.

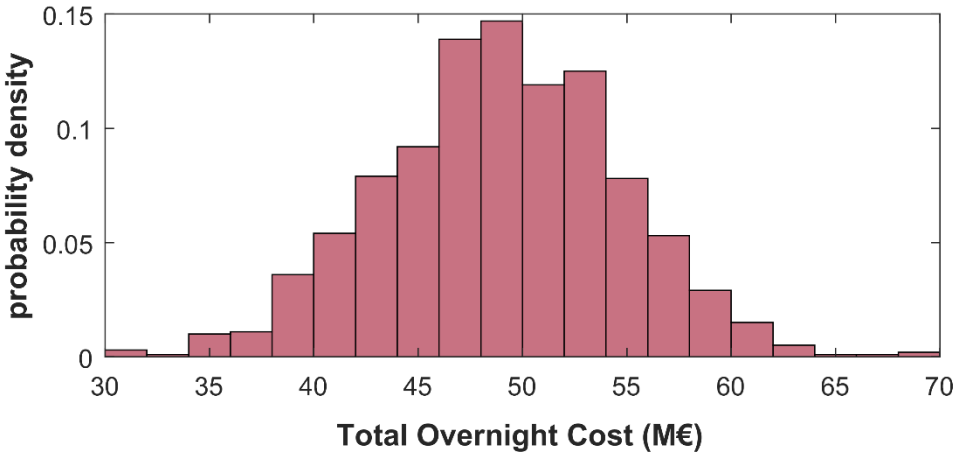

Figure 9. Total Overnight Cost (TOC) obtained from a sensitivity analysis base in random numbers.

According to the obtained results, the specific total overnight cost estimated is higher than values previously published about CaL as post-combustion CO2 capture system at large scale (~500-600MWe), which are around 1700-3000€/$KW_{e,gross}$ [39,40]. This is mainly because of the system size, since post-combustion CO_2 capture system are two order of magnitude higher than the PV-CaL system analyzed in our work. Moreover, in the PV-CaL the cost of the storage size is higher to ensure proper dispatchability. Nevertheless, as shown in Figure 9, the estimated investment cost is notably lower than the expected cost for electrochemical batteries (109M€).

Moreover, the proposed concept has a number of relevant advantages for large scale development. It is based on natural CaO precursors (such as limestone), which are among the most abundant materials in Earth. Thus, the raw material employed is widely available, non-toxic, abundant and cheap (~10 $/ton). These essential characteristics for massive energy storage make the PV-CaL concept an attractive technology for the sustainable development of PV power plants without any expected raw material competition with other applications.

CONCLUSIONS

This manuscript presents a novel concept to integrate Thermochemical Energy Storage (TCES) systems using the Calcium-Looping (CaL) cycle in PV plant (PV-CaL system) for electrical energy storage (EES). The work is focused on assessing the operation of the TCES system to address a generation strategy. Different generation strategies could be applied to the system to increase dispatchability of the PV facility. As a first conceptual approach the analysis has been focused on operation of the storage system to keep a constant power generation while the PV generation is variable. The CaL system reaches an efficiency of 39.2% which is low compared to available batteries at large scale whose efficiencies are around 60-70%. Despite this lower efficiency, the PV-CaL system presents some advantages that make it a very interesting option for sustainable and large-scale energy storage. The PV-CaL system is based on one of the most abundant materials available in nature (limestone, $CaCO_3$), which circumvents the risk of resource scarcity that may compromise the technical and economic viability of the storage system. This is one of the main advantages that this system presents over current solutions for EES based on chemical batteries. Batteries represent a suitable option for PV and wind storage; however, current materials used in commercial batteries (e.g. Li, Ni, Mn, Co) make them cost intensive whereas the amount of material needed for large-scale applications their storage capability. Another advantage of the integration of the PV-CaL system in the grid for large-

scale energy storage is that power is generated mechanically in a CO_2 turbine, a rotatory thermal engine connected to an asynchronous generator that converts mechanical power into electricity (alternating current AC power). This inertial power system results crucial as the size of the system increases due to frequency stability required to the interconnected power grid. The power block and rest of required equipment is easily scalable at the commercial level: two solid-gas reactors (e.g. fluidized bed or entrained flow reactors); two solid storage tanks ($CaCO_3$ and CaO); a vessel to store the CO_2 stream in supercritical conditions (75 bar and ambient temperature); electric heaters; equipment for solids and gas conveying; instrumentation and control system; and auxiliary systems needed for the correct operation of the system. Regarding cost analysis, very conservative values were chosen for the CaL-based storage system because of its novelty. Despite this, the estimated cost is notably lower than the typical cost of batteries, which suggests a potential further cost reduction in the next years that would increase even more the PV-CaL competitiveness. From these results it can be inferred that the proposed PV-CaL concept is an attractive technology for large-scale storage of electric energy.

ACKNOWLEDGEMENTS

This work has been supported by the European Union's Horizon 2020 research and innovation programme under grant agreement No 727348, project SOCRATCES and by the Spanish Government Agency Ministerio de Economía y Competitividad (MINECO-FEDER funds) under contracts CTQ2014-52763-C2, CTQ2017- 83602-C2 (-1-R and -2-R).

REFERENCES

[1] Sampaio PGV, González MOA. Photovoltaic solar energy: Conceptual framework. Renew Sustain Energy Rev 2017;74:590–601. doi:10.1016/j.rser.2017.02.081.

[2] International Energy Agency Photovoltaic Power Systems Programme. Snapshot of global photovoltaic markets 2016 2017:1–16. doi:ISBN 978-3-906042-42-8.

[3] (IEA) International Energy Agency. Trends 2016 in Photovoltaic Applications. Survey Report of Selected IEA Countries between 1992 and 2015. 2016.

[4] REN21. Renewables 2017: global status report. vol. 72. 2017. doi:10.1016/j.rser.2016.09.082.

[5] Jordehi AR. Parameter estimation of solar photovoltaic (PV) cells: A review. Renew Sustain Energy Rev 2016;61:354–71. doi:10.1016/j.rser.2016.03.049.

[6] Mundada AS, Shah KK, Pearce JM. Levelized cost of electricity for solar photovoltaic, battery and cogen hybrid systems. Renew Sustain Energy Rev 2016;57:692–703. doi:10.1016/j.rser.2015.12.084.

[7] Karimi M, Mokhlis H, Naidu K, Uddin S, Bakar AHA. Photovoltaic penetration issues and impacts in distribution network - A review. Renew Sustain Energy Rev 2016;53:594–605. doi:10.1016/j.rser.2015.08.042.

[8] Obi M, Bass R. Trends and challenges of grid-connected photovoltaic systems - A review. Renew Sustain Energy Rev 2016;58:1082–94. doi:10.1016/j.rser.2015.12.289.

[9] Rydh CJ, Sandén BA. Energy analysis of batteries in photovoltaic systems. Part I: Performance and energy requirements. Energy Convers Manag 2005;46:1957–79. doi:10.1016/j.enconman.2004.10.003.

[10] IRENA. Battery Storage for Renewables : Market Status and Technology Outlook. Irena 2015:60.

[11] https://www.tesla.com/es_ES/blog/Tesla-powerpack-enable-large-scale-sustainable-energy-south-australia?redirect=no n.d.

[12] Geth F, Brijs T, Kathan J, Driesen J, Belmans R. An overview of large-scale stationary electricity storage plants in Europe: Current status and new developments. Renew Sustain Energy Rev 2015;52:1212–27. doi:10.1016/j.rser.2015.07.145.
[13] Dawoud B, Amer E, Gross D. Experimental investigation of an adsorptive thermal energy storage. Int J Energy Res 2007;31:135–47. doi:10.1002/er.
[14] Flamant G, Hernandez D, Bonet C, Traverse JP. Experimental aspects of the thermochemical conversion of solar energy; Decarbonation of CaCO3. Sol Energy 1980;24:385–95. doi:10.1016/0038-092X(80)90301-1.
[15] Chacartegui R, Alovisio A, Ortiz C, Valverde JM, Verda V, Becerra JA. Thermochemical energy storage of concentrated solar power by integration of the calcium looping process and a CO2 power cycle. Appl Energy 2016;173:589–605. doi:10.1016/j.apenergy.2016.04.053.
[16] Benitez-Guerrero M, Sarrion B, Perejon A, Sanchez-Jimenez PE, Perez-Maqueda LA, Manuel Valverde J. Large-scale high-temperature solar energy storage using natural minerals. Sol Energy Mater Sol Cells 2017;168:14–21. doi:10.1016/j.solmat.2017.04.013.
[17] Obermeier J, Sakellariou KG, Tsongidis NI, Baciu D, Charalambopoulou G, Steriotis T, et al. Material development and assessment of an energy storage concept based on the CaO-looping process. Sol Energy 2017;150:298–309. doi:10.1016/j.solener.2017.04.058.
[18] Kyaw K, Matsuda H, Hasatani M. Applicability of carbonation/decarbonation reactions to high-temperature thermal energy storage and temperature upgrading. J Chem Eng Japan 1996;29:119–25. doi:10.1252/jcej.29.119.
[19] Barin I. Thermochemical data of pure substances VCH, Weinheim (1989) 1989.
[20] The Moonshot factory. Project Malta: Storing renewable energy in molten salt n.d. https://x.company/projects/malta/ (accessed November 1, 2018).
[21] Liu C, Cheng MS, Zhao BC, Dai ZM. A wind power plant with thermal energy storage for improving the utilization of wind energy. Energies 2017;10. doi:10.3390/en10122126.
[22] California ISO. Wind and Solar Curtailment April 28, 2018 2018.
[23] Alovisio A, Chacartegui R, Ortiz C, Valverde JM, Verda V. Optimizing the CSP-Calcium Looping integration for Thermochemical Energy Storage. Energy Convers Manag 2017;136:85–98. doi:10.1016/j.enconman.2016.12.093.
[24] Ortiz C, Romano MC, Valverde JM, Binotti M, Chacartegui R. Process integration of Calcium-Looping thermochemical energy storage system in concentrating solar power plants. Energy 2018;155:535–51. doi:10.1016/J.ENERGY.2018.04.180.
[25] Schorcht F, Kourti I, Scalet BM, Roudier S, Sancho LD. Best Available Techniques (BAT). Reference Document for the Production of Cement, Lime and Magnesium Oxide. 2015. doi:10.2788/12850.
[26] Ortiz C, Chacartegui R, Valverde JM, Alovisio A, Becerra JA. Power cycles integration in concentrated solar power plants with energy storage based on calcium looping. Energy Convers Manag 2017;149:815–29. doi:10.1016/j.enconman.2017.03.029.
[27] Valverde JM, Medina S. Limestone calcination under calcium-looping conditions for CO 2 capture and thermochemical energy storage in the presence of H 2 O: an in situ XRD analysis. Phys Chem Chem Phys 2017;19:7587–96. doi:10.1039/C7CP00260B.
[28] Benitez-Guerrero M, Valverde JM, Sanchez-Jimenez PE, Perejon A, Perez-Maqueda LA. Multicycle activity of natural CaCO3minerals for thermochemical energy storage in Concentrated Solar Power plants. Sol Energy 2017;153:188–99. doi:10.1016/j.solener.2017.05.068.
[29] Perejón A, Miranda-Pizarro J, Pérez-Maqueda LA, Valverde JM. On the relevant role of

solids residence time on their CO2 capture performance in the Calcium Looping technology. Energy 2016;113:160–71. doi:10.1016/j.energy.2016.07.028.
[30] Sarrion B, Valverde JM, Perejon A, Perez-Maqueda LA, Sanchez-jimenez PE. On the multicycle activity of natural limestone/dolomite for cheap, efficient and non-toxic Thermochemical Energy Storage of Concentrated Solar Power. Energy Technol 2016;4:1013–9. doi:10.1002/ente.201600068.
[31] Sarrion B, Valverde JM, Perejon A, Perez-maqueda LA, Sanchez-jimenez PE. On the multicycle activity of natural limestone/dolomite for cheap, efficient and non-toxic Thermochemical Energy Storage of Concentrated Solar Power. Energy Technol 2016. doi:10.1002/ente.201600068.
[32] National Renewable Energy Laboratory. Golden C. System Advisor Model Version 2017.1.17 (SAM 2017.1.17) n.d.
[33] Rubin ES, Short C, Booras G, Davison J, Ekstrom C, Matuszewski M, et al. A proposed methodology for CO2 capture and storage cost estimates. Int J Greenh Gas Control 2013;17:488–503. doi:10.1016/j.ijggc.2013.06.004.
[34] Aspen Technology Inc. Aspen Capital Cost Estimator: User's Guide 2012:738.
[35] Romano MC, Spinelli M, Campanari S, Consonni S, Cinti G, Marchi M, et al. The calcium looping process for low CO2 emission cement and power. Energy Procedia 2013;37:7091–9. doi:10.1016/j.egypro.2013.06.645.
[36] Politecnico di Milano – Alstom UK (CAESAR project). European best practice guidelines for assessment of CO2 capture technologies. 2011.
[37] Mantripragada HC, Rubin ES. Calcium looping cycle for CO2 capture: Performance, cost and feasibility analysis. Energy Procedia 2014;63:2199–206. doi:10.1016/j.egypro.2014.11.239.
[38] Cormos CC. Economic evaluations of coal-based combustion and gasification power plants with post-combustion CO2capture using calcium looping cycle. Energy 2014;78:665–73. doi:10.1016/j.energy.2014.10.054.
[39] Romeo LM, Abanades JC, Escosa JM, Paño J, Giménez A, Sánchez-Biezma A, et al. Oxyfuel carbonation/calcination cycle for low cost CO2capture in existing power plants. Energy Convers Manag 2008;49:2809–14. doi:10.1016/j.enconman.2008.03.022.
[40] Hanak DP, Manovic V. Economic feasibility of calcium looping under uncertainty. Appl Energy 2017;208:691–702. doi:10.1016/j.apenergy.2017.09.078.